

Article

Identification of Mutations Responsible for Improved Xylose Utilization in an Adapted Xylose Isomerase Expressing *Saccharomyces cerevisiae* Strain

Ronald E. Hector , Jeffrey A. Mertens and Nancy N. Nichols 

Bioenergy Research Unit, USDA, Agricultural Research Service, National Center for Agricultural Utilization Research, 1815 North University Street, Peoria, IL 61604, USA

* Correspondence: ronald.hector@usda.gov

Abstract: Economic conversion of biomass to biofuels and chemicals requires efficient and complete utilization of xylose. *Saccharomyces cerevisiae* strains engineered for xylose utilization are still considerably limited in their overall ability to metabolize xylose. In this study, we identified causative mutations resulting in improved xylose fermentation of an adapted *S. cerevisiae* strain expressing codon-optimized xylose isomerase and xylulokinase genes from the rumen bacterium *Prevotella ruminicola*. Genome sequencing identified single-nucleotide polymorphisms in seven open reading frames. Tetrad analysis showed that mutations in both *PBS2* and *PHO13* genes were required for increased xylose utilization. Single deletion of either *PBS2* or *PHO13* did not improve xylose utilization in strains expressing the xylose isomerase pathway. *Saccharomyces* can also be engineered for xylose metabolism using the xylose reductase/xylitol dehydrogenase genes from *Scheffersomyces stipitis*. In strains expressing the xylose reductase pathway, single deletion of *PHO13* did show a significant increase xylose utilization, and further improvement in growth and fermentation was seen when *PBS2* was also deleted. These findings will extend the understanding of metabolic limitations for xylose utilization in *S. cerevisiae* as well as understanding of how they differ among strains engineered with two different xylose utilization pathways.

Keywords: *Saccharomyces*; xylose isomerase; fermentation; strain adaptation; metabolic engineering



Citation: Hector, R.E.; Mertens, J.A.; Nichols, N.N. Identification of Mutations Responsible for Improved Xylose Utilization in an Adapted Xylose Isomerase Expressing *Saccharomyces cerevisiae* Strain. *Fermentation* **2022**, *8*, 669. <https://doi.org/10.3390/fermentation8120669>

Academic Editor:

Konstantina Kourmentza

Received: 23 September 2022

Accepted: 18 November 2022

Published: 23 November 2022

Publisher's Note: MDPI stays neutral with regard to jurisdictional claims in published maps and institutional affiliations.



Copyright: © 2022 by the authors. Licensee MDPI, Basel, Switzerland. This article is an open access article distributed under the terms and conditions of the Creative Commons Attribution (CC BY) license (<https://creativecommons.org/licenses/by/4.0/>).

1. Introduction

Biomass-derived sugars such as glucose and xylose can be metabolized by many microorganisms. However, most of them have complex genetic systems that are not amenable to the extensive genome modification required for metabolic engineering to produce biofuels and organic acids at high yields and productivities. Toxicity of lignocellulosic hydrolysates and/or end-product inhibition is also an issue with many microorganisms. Brewer's yeast, *Saccharomyces cerevisiae*, has been used extensively due to its ease of genetic modification, availability of a variety of promoters and terminators for metabolic engineering, and ability to grow anaerobically at low pH (reviewed in [1]). *S. cerevisiae* does not naturally metabolize xylose, and to overcome this limitation, strains have been engineered to express three different routes for xylose utilization [2–4]. Oxidative metabolism of xylose using the bacterial Weimberg pathway has recently been shown in *S. cerevisiae* [5]. For the two main pathways investigated in this study (oxido-reductive and isomerization), xylose is converted to xylulose-5P (X5P), which enters central metabolism through the pentose phosphate pathway (PPP) (Figure 1). The reductase/dehydrogenase pathway (XR/XDH) uses xylose reductase and xylitol dehydrogenase, typically from *Scheffersomyces stipitis*, which can lead to a redox imbalance under anaerobic conditions [6,7]. Alternatively, expression of xylose isomerase (XI) is independent of cofactors and has potential to avoid this redox imbalance [7,8]. Multiple XI genes from bacteria and anaerobic fungi have been used to metabolically engineer xylose utilization in *S. cerevisiae*. In comparison to strains

engineered with the XR/XDH pathway, most strains expressing XIs do not grow well using xylose as a carbon source, nor do they ferment xylose to ethanol without further strain modification and/or adaptation [8–17].

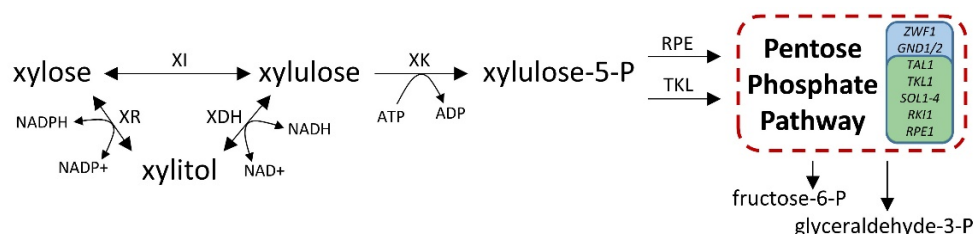


Figure 1. Xylose metabolism in engineered *Saccharomyces cerevisiae* strains. Two of the main routes for xylose metabolism are shown. A third route via the Weimberg pathway was not investigated in this study and is not shown above. Enzyme activities and genes required for xylose metabolism are: XR, D-xylose reductase (E.C. 1.1.1.21); XDH, xylitol dehydrogenase (E.C. 1.1.1.9); XI, D-xylose isomerase (E.C. 5.3.1.5); XK, xylulokinase (E.C. 2.7.1.17); TKL, transketolase (E.C. 2.2.1.1); RPE, ribulose 5-phosphate-3-epimerase (E.C. 5.1.3.1). Pentose phosphate pathway (PPP) genes, shaded in blue (oxidative branch) and green (non-oxidative branch), catalyze a series of carbon-transfer reactions resulting in fructose-6-P and glyceraldehyde-3-P, which can be further metabolized via glycolysis.

Numerous studies have shown it is possible to increase xylose utilization in engineered strains by adaptive laboratory evolution. However, many of these studies do not identify the causative mutations [18–30]. Studies that do identify genetic changes in strains evolved for increased xylose fermentation overwhelmingly show changes associated with increased activity of the PPP, irrespective of route used to convert xylose to X5P. Loss of *PHO13* function is commonly seen in adapted strains, as *PHO13* deletion increases PPP activity [15,31,32]. Aside from increasing PPP activity, *PHO13* deletion also appears to alleviate ATP depletion, which is putatively caused by futile cycling around xylulose and X5P [33]. Many adaptive evolution studies aimed at improving xylose metabolism also start with strains overexpressing either the PPP gene *TAL1* (encodes transaldolase) or overexpressing multiple PPP genes. For genetic studies on strains overexpressing PPP genes, mutation to *PHO13* was either not identified [14,17,34–39], or, *PHO13* deletion was shown to negatively affect xylose utilization [22,40]. Conversely, strains without PPP overexpression often identify *PHO13* mutations or deletion as beneficial [15,22,31–33].

When starting with low-copy xylose isomerase, adapted strains frequently show increased copy number of the XI gene. Starting with the Brazilian industrial ethanol production strain PE-2, dos Santos et al. (2016) integrated *Orpinomyces* XI and extra *XKS1* copies, as well as integrated PPP genes (*TAL1*, *TKL1*, *RPE1*, *RKI1*), and deleted *GRE3* [35]. Genome sequencing of the evolved strain revealed approximately 26 copies of the XI gene, as well as additional mutations in *ISU1* and *SSK2*. Several other studies with adapted strains also identified increased XI gene copy number ranging up to 36-fold [14,36,39,41], highlighting the need for increased XI activity for growth on xylose.

Previously, we discovered a xylose isomerase from the rumen bacterium *Prevotella ruminicola* TC2-24 and expressed both the XI and XK enzymes from this bacterium in *S. cerevisiae* and evaluated its ability to grow on xylose [16]. Xylose fermentation was initially poor, and the specific growth rate for aerobic xylose cultures was $0.06 \text{ h}^{-1} \pm 0.005$. Adaptive laboratory evolution was performed for ca. 40 generations under microaerobic conditions and the resulting strain, YRH1114, had a 3.8-fold increase in aerobic growth rate to $0.23 \text{ h}^{-1} \pm 0.024$. Under anaerobic conditions, xylose consumption and final ethanol concentration increased 2.7-fold and 3.3-fold, respectively, in the adapted strain. Xylitol yield also decreased 1.7-fold and ethanol yield increased 1.2-fold, suggesting that xylose was more efficiently fermented to ethanol in the adapted strain.

The goal of this study was to identify the genetic changes in the adapted strain that are responsible for increased xylose utilization. Of the seven ORF mutations discovered

within the genome of the adapted haploid strain, two mutations are required for increased xylose fermentation. Strains containing individual mutation, or gene deletion, of either *PBS2* or *PHO13* did not grow well on xylose medium. Also, the requirement for both mutations is specific for the XI pathway, as strains expressing the XR/XDH pathway for xylose metabolism demonstrated a significant increase in xylose utilization with only the *PHO13* mutation.

2. Materials and Methods

2.1. Strains, Media, and General Methods

Media preparation, cell growth, transformation, and statistical analyses were performed as previously described [42]. All plasmids and microorganisms used in this study are listed in Tables 1 and 2, respectively. DNA oligonucleotides used in this study are listed in Supplementary Table S1. Methods used to construct plasmids for expressing *PBS2* and *PHO13* and constructing strains with *PBS2* and *PHO13* deletions are also described in the Supplemental Materials. Adaptation of *S. cerevisiae* for increased xylose fermentation was described previously [16]. In short, to create the adapted YRH1114 strain, the unadapted haploid strain YRH631 (CEN.PK2-1C with plasmid-based expression of codon-optimized *P. ruminicola* XI and XK genes) was serially passaged every seven days for six weeks. To maintain microaerobic conditions, 100 mL cultures were incubated at 30 °C in stoppered 125 mL Erlenmeyer flasks. For each passage, cells from the previous culture were diluted to an OD₆₀₀ of 0.1 in YP medium supplemented with 50 g/L of D-xylose. Ethanol, xylitol, and residual xylose concentrations were measured at the end of each passage. After passage six, ca. 40 generations, ethanol production ceased to increase.

Table 1. Plasmids used in this study.

Plasmid #	Description	Reference
pRS413	pBluescript II SK+, <i>HIS3</i> , <i>CEN6</i> , <i>ARSH4</i>	[43]
pRS414	pBluescript II SK+, <i>TRP1</i> , <i>CEN6</i> , <i>ARSH4</i>	[43]
pRS415	pBluescript II SK+, <i>LEU2</i> , <i>CEN6</i> , <i>ARSH4</i>	[43]
pRS416	pBluescript II SK+, <i>URA3</i> , <i>CEN6</i> , <i>ARSH4</i>	[43]
pRS426	pBluescript II SK+, <i>URA3</i> , 2 μ origin	[43]
pGALHOT	P_{GAL10} <i>HO</i> , <i>TRP1</i> , <i>CEN4</i>	[44]
pRH164 ^A	pRS414 + P_{HXT7} —MCS— T_{HXT7}	[45]
pRH167 ^A	pRS426 + P_{HXT7} —MCS— T_{HXT7}	[45]
pRH274 ^B	pRS416 + P_{PGK1} - <i>SsXYL1</i> - T_{PGK1} ; P_{ADH1} - <i>SsXYL2</i> - T_{ADH1} ; P_{HXT7} - <i>ScXKS1</i> - T_{HXT7}	[46]
pRH384	pRH167 + Xylose Isomerase ^C cloned into the MCS	[16]
pRH385	pRH164 + Xylulokinase ^C cloned into the MCS	[16]
pRH544	Xylulokinase ^C plasmid pRH385 rescued from YRH1137	This study
pRH545	Xylose isomerase ^C plasmid pRH384 rescued from YRH1138	This study
pRH1000	pRS415 + P_{PBS2} - <i>PBS2</i> - T_{PBS2}	This study
pRH1011	pRS413 + P_{PHO13} - <i>PHO13</i> - T_{PHO13}	This study

^A The *HXT7* promoter (P_{HXT7}) used in this work refers to the truncated, constitutive promoter, containing 390 nucleotides 5' of the *HXT7* ORF [47]. ^B *SsXYL1* and *SsXYL2* were cloned from *Scheffersomyces stipitis*. ^C Xylose isomerase and xylulokinase genes were from *Prevotella ruminicola* TC2-24 and were optimized for expression in *S. cerevisiae* [16].

2.2. Growth Analysis

Cells were grown in xylose medium using the Bioscreen CTM automated microbiology growth curve analysis system (Growth Curves USA; Piscataway, NJ, USA), which features 100 micro-well culture plates. Growth assays were performed essentially as described in [16]. Each strain was analyzed in at least quadruplicate using separate biological replicates. Cell mass (OD₆₀₀) was determined by converting the wideband OD (WB) values from the Bioscreen CTM as described in [16].

Table 2. Microorganisms used in this study.

Strain #	Genotype/Description	Reference
NEB 5- α	<i>E. coli</i> <i>fluA2Δ(argF-lacZ)U169 phoA glnV44 f80Δ(lacZ)M15 gyrA96 recA1 relA1 endA1 thi-1 hsdR17</i>	NEB
CEN.PK2-1C	<i>S. cerevisiae</i> <i>MATα, ura3-52, trp1-289, leu2-3,112, his3Δ 1, MAL2-8^c; SUC2</i>	Euroscarf
YRH631	CEN.PK2-1C + [pRH384, pRH385] [also carries <i>ste24^{L418F}</i>]	[16]
YRH1114	YRH631 microaerobically adapted on xylose medium	[16]
YRH1136	YRH1114 without pRH384 and pRH385	[16]
YRH1137	YRH1114 with only pRH385 (xylulokinase plasmid)	This study
YRH1138	YRH1114 with only pRH384 (xylose isomerase plasmid)	This study
YRH1169	YRH1136 + [pRH544, pRH545]	This study
YRH1170	YRH1136 + [pRH384, pRH385]	This study
YRH1563	YRH631 with <i>pho13Δ::HIS3</i>	This study
YRH1188	CEN.PK2-1C + [pRH384, pRH385], remade to correct <i>STE24</i>	This study
YRH1911	YRH1136 + [pGAL-HOT] (HO expression vector for switching mating type)	This study
YRH1932	YRH1114 with fixed genomic <i>PBS2</i>	This study
YRH1934	YRH1114 with fixed genomic <i>PBS2</i> + [pRH384, pRH385]	This study
YRH1954	YRH1136 with mating type switched to <i>MATα</i>	This study
YRH1955	YRH1954 + [pRS413] (empty <i>HIS3</i> vector for diploid selection)	This study
YRH1966	YRH1114 + [pRS415] (empty <i>LEU2</i> vector control)	This study
YRH1968	YRH1114 + [pRH1000] (<i>PBS2</i> expression vector)	This study
YRH1981	YRH1955 X YRH631 (heterozygous diploid): <i>MATα/MATα, PBS2/pbs2, SAS3/sas3, PHO13/pho13, PHO81/pho81, HSP104/hsp104, ste24/ste24</i> + [pRH384, pRH385]	This study
YRH1982	YRH1955 X YRH1114 (homozygous diploid): <i>MATα/MATα, pbs2/pbs2, sas3/sas3, pho13/pho13, pho81/pho81, hsp104/hsp104, ste24/ste24</i> + [pRH384, pRH385]	This study
YRH1994	YRH1981 tetrad #1 spore A	This study
YRH1995	YRH1981 tetrad #1 spore B	This study
YRH1996	YRH1981 tetrad #1 spore C	This study
YRH1997	YRH1981 tetrad #1 spore D	This study
YRH2002	YRH1981 tetrad #3 spore A	This study
YRH2003	YRH1981 tetrad #3 spore B	This study
YRH2004	YRH1981 tetrad #3 spore C	This study
YRH2005	YRH1981 tetrad #3 spore D	This study
YRH2006	YRH1981 tetrad #4 spore A	This study
YRH2007	YRH1981 tetrad #4 spore B	This study
YRH2008	YRH1981 tetrad #4 spore C	This study
YRH2009	YRH1981 tetrad #4 spore D	This study
YRH2010	YRH1981 tetrad #5 spore A	This study
YRH2011	YRH1981 tetrad #5 spore B	This study
YRH2012	YRH1981 tetrad #5 spore C	This study
YRH2013	YRH1981 tetrad #5 spore D	This study
YRH2014	YRH1981 tetrad #6 spore A	This study
YRH2015	YRH1981 tetrad #6 spore B	This study
YRH2016	YRH1981 tetrad #6 spore C	This study
YRH2017	YRH1981 tetrad #6 spore D	This study
YRH2021	YRH631 with <i>pbs2Δ::LEU2</i>	This study
YRH2022	YRH631 with <i>pbs2Δ::LEU2, pho13Δ::HIS3</i>	This study
YRH2040	CEN.PK2-1C + [pRH274] (XR/XDH/XK plasmid)	This study
YRH2042	YRH1114 + [pRS413] (empty <i>HIS3</i> vector control)	This study
YRH2043	YRH1114 + [pRH1011] (<i>PHO13</i> expression vector)	This study
YRH2044	YRH1114 + [pRS413, pRS415] (empty <i>HIS3, LEU2</i> vector controls)	This study
YRH2045	YRH1114 + [pRH1000, pRH1011] (<i>PHO13</i> and <i>PBS2</i> expression vectors)	This study
YRH2053	CEN.PK2-1C with <i>pbs2Δ::LEU2</i> + [pRH274] (XR/XDH/XK plasmid)	This study
YRH2054	CEN.PK2-1C with <i>pho13Δ::HIS3</i> + [pRH274] (XR/XDH/XK plasmid)	This study
YRH2055	CEN.PK2-1C with <i>pbs2Δ::LEU2, pho13Δ::HIS3</i> + [pRH274] (XR/XDH/XK plasmid)	This study
YRH2056	CEN.PK2-1C with <i>pbs2Δ::LEU2</i> + [pRH384, pRH385]	This study
YRH2057	CEN.PK2-1C with <i>pho13Δ::HIS3</i> + [pRH384, pRH385]	This study
YRH2058	CEN.PK2-1C with <i>pbs2Δ::LEU2, pho13Δ::HIS3</i> + [pRH384, pRH385]	This study

2.3. Genome Sequencing and Analysis

Genomic DNA isolation, library preparation, and sequencing were performed as previously described [48]. In short, sequencing libraries were constructed from isolated genomic DNA using the Nextera XT Library prep kit following the manufacturer protocol (Illumina, San Diego, CA, USA). The library samples were processed for sequencing and loading using the MiSeq Reagent Kit v3 (Illumina; San Diego, CA, USA) and run per the

manufacturer protocol on the MiSeq system with a maximum read length of 2×300 bp. Sequencing reads were trimmed to eliminate adaptors, low quality ($Q < 20$) bases, and ambiguous nucleotides, and reads were filtered to remove bacterial and human DNA contaminants using CLC Genomics Workbench version 20.0.4 (Qiagen; Germantown, MD, USA). Sequence read depth for strains CEN.PK2-1C, YRH1114, and YRH1136 was 85X, 63X, and 30X, respectively. Reads were deposited in the GenBank SRA database under BioProject number PRJNA877627. Trimmed reads of the unadapted CEN.PK2-1C reference strain, the adapted strain containing the plasmid-based xylose utilization pathway, YRH1114, and the strain cured of the xylose pathway plasmids, YRH1136, were mapped to the annotated genome sequence of the *Saccharomyces cerevisiae* reference strain, CEN.PK113-7D (NCBI BioProject PRJNA393501) using the CLC Genomics Workbench default parameters. Duplicate reads were removed, and local realignments were performed to improve mapping accuracy. Variants (i.e., SNPs and INDELS) of each mapped strain were called using the default parameters in CLC Genomics Workbench. The variants of YRH1114 and YRH1136 were then filtered to remove the variants found in the wild-type CEN.PK2-1C strain. The variant list was then filtered to remove variants with low coverage resulting in 158 variants in the adapted strains. Mutations with potential functional consequence were determined using the GO Enrichment Analysis tool in CLC Genomics Workbench package, leaving a final list of 7 variants.

2.4. Mating-Type Testing and MAT Switching

The plasmid pGAL-HOT, containing the *HO* gene behind a galactose-induced promoter and *TRP1* marker, was used to switch the mating type of the haploid strains. After growing overnight in YP + sucrose (20 g/L), YRH1911 cells were resuspended in YP + galactose (20 g/L) and incubated (30 °C, 250 rpm). After 4 h of induction, cells were diluted and plated to obtain approximately 100–200 cells per YPD plate. Mating type was confirmed by multiplex PCR as described in [49]. A *MATa* isolate of the adapted strain was allowed to lose the pGAL-HOT vector, by passage without selection, to generate YRH1954. YRH1955 was generated by transforming YRH1954 with an empty pRS413 (*HIS3*) to facilitate diploid selection. Mating pairs (YRH1955 X YRH631 and YRH1955 X YRH1114) were then patched together on YPD plates to allow mating. After incubation for 6 h at 30 °C, cells were transferred to SD-Ura-Trp-His plates to select only for diploid cells. Mating type was again confirmed by multiplex PCR as described in [49], with diploids showing the presence of both *MATa* and *MAT α* specific genes at the mating type locus.

2.5. Tetrad Dissection

The heterozygous diploid strain YRH1981 (from YRH1955 X YRH631 mating) was grown overnight in synthetic complete medium with 20 g/L glucose (SD-Ura-Trp) to an $OD_{600} \sim 0.8$. Cells were washed once with sterile water and resuspended in SD-Ura-Trp and allowed to grow overnight in a roller drum at 30 °C. Cells were washed twice with sterile water and resuspended in 1% potassium acetate sporulation medium and incubated at 30 °C for 3 to 5 days. Sporulated cells (500 mL) were washed twice with sterile water and resuspended with 50 μ L of digestion buffer (1 mL of 1M sorbitol and 0.5 μ L of zymolyase (5 U/mL), ZymoResearch; Irvine, CA, USA). Tetrads were incubated in digestion buffer at 37 °C. After 30 min, 1 mL of sterile water was added, and the tetrads were stored on ice to stop digestion. A 20 μ L volume of digested tetrads was transferred to an SD-Ura-Trp plate for dissection. Tetrads were dissected using a SporePlay dissection microscope (Singer Instruments; Somerset, UK). Plates containing the spores were incubated at 30 °C. Each haploid was tested to determine mating type, SNP presence, and ability to grow on xylose medium.

2.6. SNP PCR

The presence or absence of each SNP was determined using a one-step PCR assay as described in [50]. Primers were designed with a common mismatched nucleotide at position -2 . Primers for amplification of the wild-type and SNP variants have the SNP mutation as the

final 3' nucleotide in the primer (position 0). The wild-type primer results in a product only if the wild-type gene is present. Conversely, the SNP primer only results in a PCR product from the mutated gene. Two separate PCR assays using wild-type or SNP primers with a common reverse primer were performed for each haploid from tetrad dissection.

2.7. Batch Fermentation

Xylose fermentation was performed using 50 mL cultures of YP medium supplemented with 50 g/L xylose in a 125 mL Erlenmeyer flask incubated at 30 °C with shaking at 150 RPM for 4 days. Cells for inoculation were grown to mid-log phase in either SD-Ura-Trp or SD-Ura medium, depending on the strain, to maintain selection for plasmids. YP5X cultures were inoculated to a starting OD₆₀₀ of ~1.0. Flasks were sealed with a rubber stopper pierced with a 20-gauge needle with glass wool placed at one end to restrict ingress of air and enable release of CO₂. Samples were taken at various timepoints to determine cell mass (OD₆₀₀), xylose, and fermentation products (by high-performance liquid chromatography, HPLC as previously described [51]). Fermentation experiments were performed using three biological repeats and all fermentation data calculations (i.e., yields, rates, and carbon recoveries) were performed as previously described [16]. Probability analyses were performed using Student's t test with a two-tailed distribution. Values with $p < 0.05$ were considered significant for this study. Statistical analysis was performed using Microsoft Excel. Cell dry weight (CDW) was calculated using an OD-to-CDW conversion factor for the yeast strains used in this study ($CDW_{\text{haploid}} = 0.65 \pm 0.003$ g/L/OD₆₀₀, $CDW_{\text{diploid}} = 0.73 \pm 0.007$ g/L/OD₆₀₀). The conversion factor was determined by drying cells at differing OD to constant weight at 100 °C. Cells were washed two times with distilled water prior to drying. OD₆₀₀ was measured using a BioMate 3S spectrophotometer (Thermo Fisher Scientific Inc.; Waltham, MA, USA).

3. Results and Discussion

3.1. Genome Sequence Analysis of the Adapted Strain

Gene amplification is commonly observed in adapted strains [52–54], and several studies starting with integrated xylose isomerase indicate that increased copy number of the gene is essential for increased xylose utilization [14,35,36,39,41]. In this study, high copy number was gained by expressing the XI gene from a high-copy number plasmid. XK was also expressed from a separate low-copy plasmid because, while elevated XK levels are required to increase xylose fermentation, excess expression of XK in several studies has been shown to be detrimental to xylose (and xylulose) fermentation [55–59].

First, we determined if the XI gene was integrated into the genome. Starting with the adapted YRH1114 strain, progeny strains were generated that had lost one or both vectors for expressing either the XI or XK genes. Strains that lost the high-copy XI vector also lost the ability to grow on xylose, suggesting that copies of the XI gene did not integrate into the genome. Increased ability to grow on xylose was observed when new plasmids for expressing the XI and XK were reintroduced into the adapted strain lacking its original XI/XK plasmids. DNA sequencing of the rescued expression plasmids also confirmed that mutations were not present in the plasmid sequence. The sum of these results indicated that the causative mutations required for increased growth on xylose occurred within the native genome and not as a result of genome integrated XI or mutation(s) occurring within the expression vectors. Aside from expected regions of high coverage (i.e., rDNA, Ty elements, and sub-telomeric), genome sequencing and read-depth analysis of the adapted YRH1114 strain did not reveal additional regions with increased copy number. Further analysis for insertions/deletions (INDELs) and single-nucleotide polymorphisms (SNPs) did show the presence of seven SNPs located in open reading frames that were not present in the CEN.PK2-1C genome (Table 3).

Table 3. SNPs identified in the adapted YRH1114 strain.

GENE	SNP	ORF	Chromosome	Function *
<i>SAS3</i>	G ₇₃₃ to T	E ₂₄₅ X	2-L	Histone acetyltransferase subunit of NuA3 complex that catalyzes acetylation of histone H3
<i>YBR225W</i>	C ₁₈₃₉ to T	N ₆₃₁ (Silent)	2-R	Protein whose biological role and cellular location are unknown
<i>PHO13</i>	G ₆₂₂ to T	G ₂₀₈ C	4-L	Alkaline phosphatase specific for <i>p</i> -nitrophenyl phosphate
<i>PHO81</i>	C ₃₁₈₂ to T	P ₁₀₆₁ L	7-R	Cyclin-dependent protein serine/threonine kinase inhibitor involved in phosphate metabolism
<i>PBS2</i>	T ₁₀₀₈ to A	L ₃₆₃ X	10-L	MAP kinase kinase of the HOG signaling pathway; activated under severe osmotic stress
<i>STE24</i>	C ₁₂₅₂ to T	L ₄₁₈ F	10-R	Highly conserved zinc metalloprotease; component of the ER quality control mechanism that removes faulty proteins clogging translocation channels
<i>HSP104</i>	T ₁₈₉₂ to C	L ₆₃₁ S	12-L	Adenosine-binding protein chaperone involved in protein folding

* Annotation from the *Saccharomyces* Genome Database (<https://www.yeastgenome.org/>, accessed on 26 August 2022).

Of the seven SNPs identified in YRH1114, two genes had been discovered in other adapted strains. Transposon mutagenesis and selection for improved growth on xylose led to the discovery of strains with transposons inserted into the *PHO13* gene [32]. Separately, Kim et al., (2013) identified two additional *PHO13* mutations (i.e., *pho13*^{G166R} and *pho13*^{G253D}) in strains evolved for improved xylose fermentation [33]. In both studies, the *PHO13* mutations were hypothesized to result in lost or decreased Pho13p function, and analysis of strains with targeted deletion of *PHO13* supported their hypotheses. Additional studies of strains with targeted *PHO13* deletion showed increased carbon flux through the PPP, which is essential for xylose metabolism [15,31,32]. Like the previously discovered *pho13* mutant alleles mentioned above, the *pho13*^{G208C} mutation identified in our adapted strain resulted in an altered glycine residue. Glycine residues influence the formation of short loops [60]. Further inspection of the location of the *pho13*^{G166R}, *pho13*^{G253D}, and *pho13*^{G208C} mutations with respect to predicted protein structure [61,62] showed that the mutated glycine residues were all located at the start of a short loop between two secondary protein structures. It is possible that mutation of the glycine residues in these alleles disrupts loop formation, resulting in altered protein folding and decreased function. Regarding the other gene discovered in another adapted strain, *ask10*^{M475R} and *ask10*Δ mutations were identified that resulted in upregulated *HSP104* levels [37]. Both *ask10* mutants, as well as *HSP104* overexpression, were suggested to increase XI activity by facilitating protein folding [37]. The five other genes listed in Table 3 have not been previously associated with xylose metabolism.

3.2. Determination of Phenotype Dominance

To identify which of the seven mutations were phenotypic, we generated heterozygous (unadapted/adapted) diploids to first determine if improved xylose utilization was dominant or recessive. The mating type of the adapted haploid strain YRH1114 was switched from *MATa* to *MATα* and the adapted *MATα* strain was mated to an unadapted parent strain YRH631 (*MATa*) to create the heterozygous diploid strain YRH1981. The *MATα* version of YRH1114 was mated to the *MATa* YRH1114 strain to generate the homozygous diploid strain YRH1982. Both diploid strains were grown on xylose and compared to the original unadapted and adapted haploid strains (Figure 2). The heterozygous diploid YRH1981 grew as poorly as the unadapted YRH631 strain and the homozygous diploid

YRH1982 grew nearly as well as the adapted haploid strain, indicating that the genetic changes were recessive.

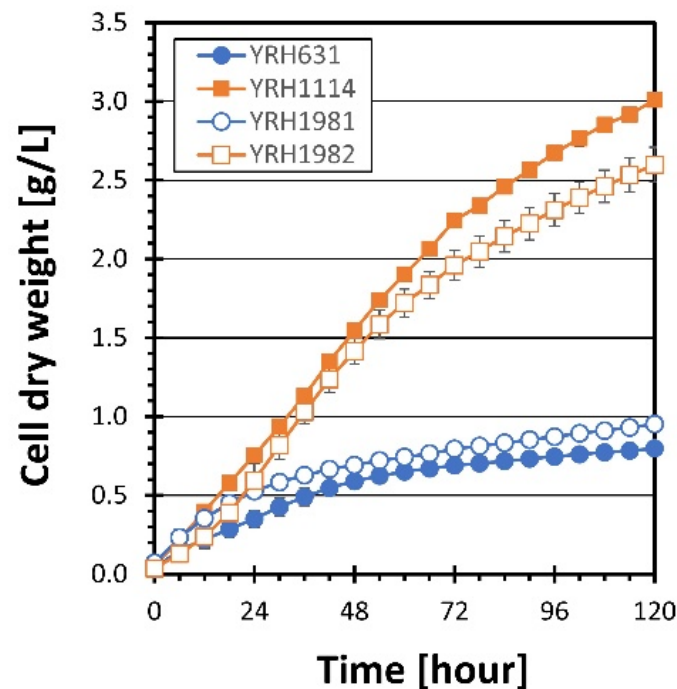


Figure 2. Comparison of growth on xylose medium. Homozygous diploid (YRH1982 ◻) and heterozygous diploid (YRH1981 ◻) strains were grown on YP medium + 50 g/L xylose and compared to the unadapted haploid (YRH631 ●) and adapted haploid (YRH1114 ■) strains. Cell dry weight was used to measure cell mass instead of OD₆₀₀ to account for differences in dry weight per OD₆₀₀ between haploid and diploid strains. Plots are the average values from at least triplicate cultures. Error bars show standard deviations.

3.3. Tetrad Dissection to Identify Causative Mutations

Most of the SNPs were located on different chromosomes, and mutations located on the same chromosome appeared on opposite arms of the chromosome (Table 3). Since none of the SNPs were closely linked, haploid spores from the heterozygous diploid were analyzed to determine which SNPs were associated with improved growth on xylose medium. Heterozygous diploid strain YRH1981 was sporulated and tetrads with re-assorted wild-type and SNP combinations were dissected onto SD-Ura-Trp plates to maintain selection for the XI and XK expression plasmids (Figure 3A). Growth of the haploids was compared in xylose cultures (Figure 3B). The presence of the expected SNP in each haploid was confirmed using a PCR-based SNP detection assay; the results of the tetrad analysis are listed in Table 4.

Each haploid strain from the tetrad analysis that grew well in xylose medium carried both *pho13*^{G208C} and *pbs2*^{L363X} mutations; these mutations were identified as likely candidates for increased growth on xylose seen in these strains. None of the haploid strains carrying just one of these mutations was able to grow as well on xylose medium, further suggesting that both *pho13*^{G208C} and *pbs2*^{L363X} mutations are required. The *pbs2*^{L363X} mutation results in leucine-to-stop change in the middle of protein, likely rendering it non-functional. Additionally, since loss-of-function mutation, or deletion, of *PHO13* has previously been shown to increase xylose utilization [15,31–33], the *pho13*^{G208C} mutation in our adapted strain is also likely non-functional. The ability of multiple haploid strains with these two mutations to grow well in xylose medium, regardless of other SNPs, also indicated that the SNPs and INDELS located in intergenic regions do not play a significant role in xylose utilization.

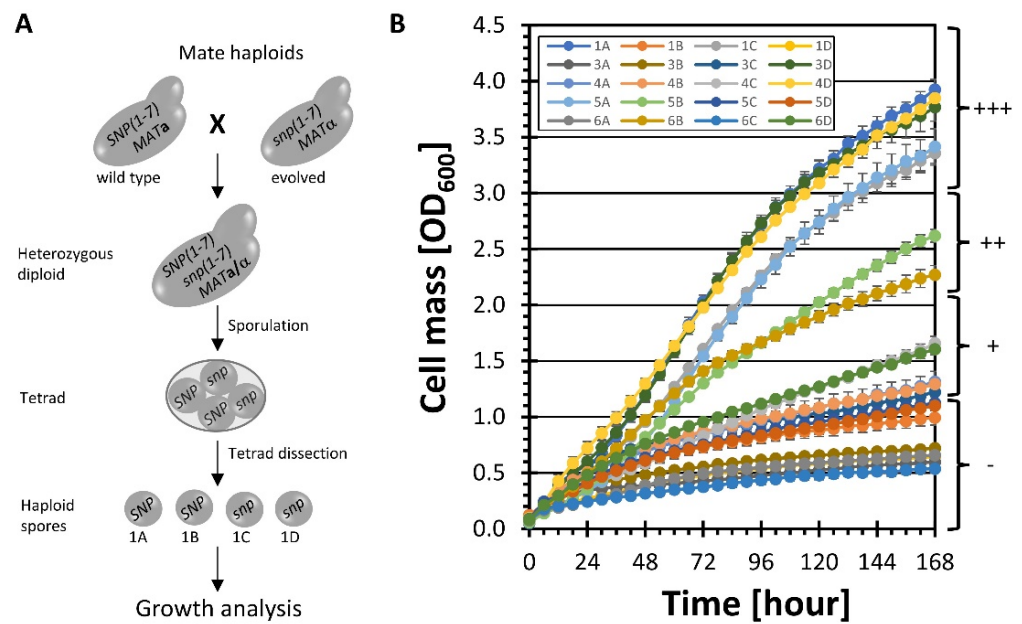


Figure 3. Identification of mutations present in strains with improved growth on xylose. **(A)** Sporulation of the heterozygous diploid strain YRH1981 was performed to re-distribute SNPs among haploid spores. **(B)** Each haploid spore was grown on YP medium + 50 g/L xylose to identify strains that maintained the ability to grow well on xylose. Plots are the average values from at least three biological replicates. Error bars show standard deviations. For lower OD values, error bars are smaller than the symbol. Growth ratings (−, +, ++, +++) are used in Table 4.

Table 4. Tetrad analysis.

Strain	Tetrad	MAT	Growth *	PBS2 **	PHO13	SAS3	HSP104	PHO81	STE24
YRH 1994	1A	α	+++	−	−	+	−	+	−
YRH 1995	1B	a	−	+	+	−	+	−	−
YRH 1996	1C	α	+++	−	−	+	−	+	−
YRH 1997	1D	a	−	+	+	−	+	+	−
YRH 2002	3A	a	−	+	−	+	+	−	−
YRH 2003	3B	α	−	+	+	−	+	+	−
YRH 2004	3C	a	+	−	+	−	−	−	−
YRH 2005	3D	α	+++	−	−	+	−	+	−
YRH 2006	4A	a	+	+	+	+	−	−	−
YRH 2007	4B	a	+	−	+	−	−	+	−
YRH 2008	4C	α	+	+	−	−	+	+	−
YRH 2009	4D	α	+++	−	−	+	+	−	−
YRH 2010	5A	α	+++	−	−	+	+	+	−
YRH 2011	5B	α	++	+	−	−	+	−	−
YRH 2012	5C	a	+	+	+	+	−	−	−
YRH 2013	5D	a	+	−	+	−	−	−	−
YRH 2014	6A	a	−	−	+	−	+	+	−
YRH 2015	6B	α	++	+	−	−	−	−	−
YRH 2016	6C	a	−	+	−	+	+	+	−
YRH 2017	6D	α	+	−	+	+	−	−	−

* See Figure 3B for growth ratings. ** (+) indicates presence of the WT allele while (−) indicates presence of the mutant allele.

3.4. Validation of PBS2 and PHO13 Genes

Since results from the heterozygous diploid strain indicated that the mutations were recessive, we next expressed wild-type *PBS2* and *PHO13* genes in the adapted strain and compared growth to that of the original adapted strain YRH1114, as well as the adapted strain with empty vector controls (i.e., YRH1966, YRH2042, and YRH2044). Expression of

both *PBS2* and *PHO13*, either separately or combined, reduced growth on xylose medium, but not to the extent of the unadapted strain YRH631 (Figure 4A). One possible explanation is that episomal expression of the genes does not adequately replicate the expression level from their native genomic locations. Additionally, it was possible that one of the SNPs was exerting a semi-dominant effect in the presence of the wild-type gene.

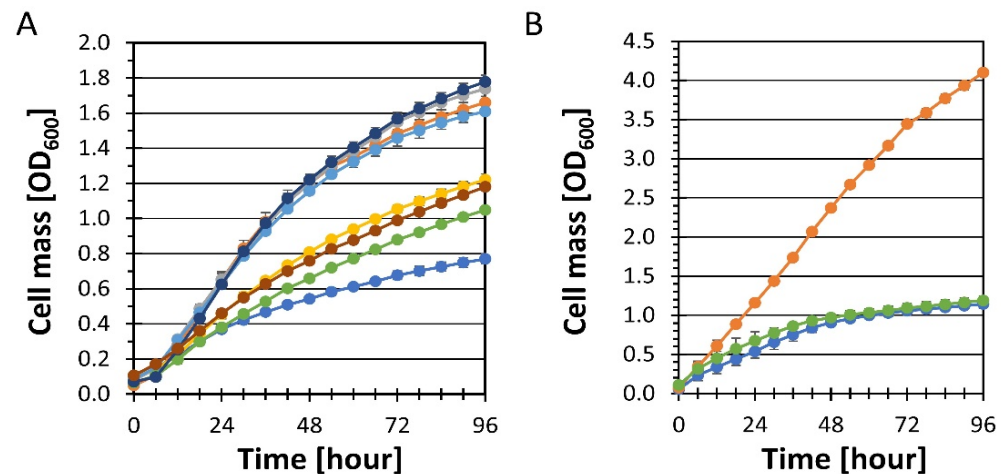


Figure 4. Expression of *PBS2* and *PHO13* in the adapted YRH1114 strain. **(A)** Plasmid-based expression. Cells were grown on synthetic drop-out medium + 50 g/L xylose (SC5X). Amino acids were supplemented as required to maintain selection of empty vector control plasmids and *PBS2* and *PHO13* expression plasmids. Plasmid-based expression of *PBS2* or *PHO13* reduced growth on xylose. **(B)** Genome replacement of the *pbs2*^{L363X} allele. Strain YRH1934, with genomic *pbs2*^{L363X} allele replaced with wild-type *PBS2* in YRH1114, was grown on xylose (YP5X medium) and compared to YRH1114 and YRH631. Plots are the average values from at least triplicate cultures. Error bars show standard deviations. Strain description: Panels **(A,B)** — YRH631 (unadapted strain), — YRH1114 (adapted strain); Panel **(A)** — YRH1966 (YRH1114 + empty vector), — YRH1968 (YRH1114 + *PBS2* plasmid), — YRH2042 (YRH1114 + empty vector), — YRH2043 (YRH1114 + *PHO13* plasmid), — YRH2044 (YRH1114 + empty vectors), — YRH2045 (YRH1114 + *PBS2* and *PHO13* plasmids); Panel **(B)** — YRH1934 (YRH1114 + corrected genomic *PBS2*).

The kinase domain of Pbs2p encompasses amino acids 360 to 688, and truncation mutations of *pbs2p* lacking the kinase domain still show Hog1p binding activity [63]. *HOG1* deletion has been shown to increase xylose utilization [17]; the *pbs2*^{L363X} allele likely exerts its function through Hog1p (see Results and Discussion, Section 3.8). Thus, it is possible that the *pbs2*^{L363X} allele, which creates a stop codon at amino acid 363, could interfere with wild-type *PBS2*. When both *PBS2* and *pbs2*^{L363X} are expressed in the same cell, the shortened, non-phosphorylating mutant *pbs2p* could compete with wild-type Pbs2p for Hog1p binding, resulting in decreased Hog1p phosphorylation. To test this possibility, the wild-type *PBS2* gene was re-integrated into the adapted strain YRH1114 at its normal location to make strain YRH1934, thus removing any expression of the mutant *pbs2p*. Strain YRH1934, with only the *pbs2*^{L363X} mutation replaced with *PBS2* in the genome and all other SNPs present, had a growth pattern identical to the unadapted strain (Figure 4B). These data suggest that for strains expressing the XI pathway, mutation in both *PBS2* and *PHO13* genes is required to improve growth on xylose. The data also suggest that the *pbs2*^{L363X} allele is semi-dominant when present with the wild-type *PBS2* allele.

3.5. Analysis of Strains with *PBS2* and *PHO13* Deletions

While results from the heterozygous diploid strain suggested that at least one of the two mutations responsible for improved growth on xylose was recessive, it was not clear whether complete loss of function could also improve growth on xylose, or if partial function of the mutant allele was required. Starting with the unadapted YRH631 parental

strain, we next deleted *PBS2* and *PHO13*, separately or together. Using YRH631, single deletions of *PBS2* or *PHO13* were unable to improve growth on xylose. In contrast, deletion of both *PBS2* and *PHO13* did improve xylose growth (Figure 5A). Upon further analysis of SNPs in YRH1114 versus YRH631, we discovered that the *ste24*^{L418F} SNP was present in the parental YRH631 background, and thus propagated throughout the haploids obtained from tetrad dissection. To rule out any involvement of *ste24*^{L418F} for improving growth on xylose, we recreated the *PBS2* and *PHO13* deletions in the parent CEN.PK2-1C background with wild-type *STE24* and re-transformed the strains with XI and XK expression vectors. No difference in growth was observed when using the CEN.PK2-1C background (Figure 5B) compared to strains generated from the YRH631 parent. These results indicated that the *ste24*^{L418F} mutation did not facilitate growth on xylose and that the growth advantage on xylose medium stems from loss of function of both *PBS2* and *PHO13*.

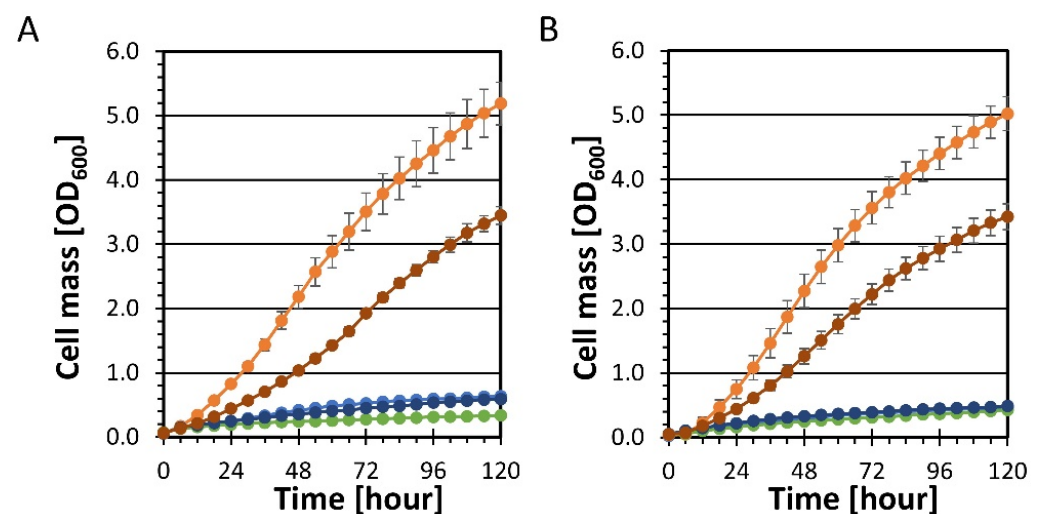


Figure 5. Deletion of both *PBS2* and *PHO13* are required for enhanced growth on xylose. (A) Growth curves for strains with *PBS2* or *PHO13* deletion in the unadapted parent YRH631. (B) Growth curves for strains with *PBS2* or *PHO13* deletion in the unadapted CEN.PK2-1C strain. YP5X medium was used for both (A,B). Plots are the average values from at least triplicate cultures. Error bars show standard deviations. Strain description: Panels (A,B) ● YRH631 (unadapted strain), ● YRH1114 (adapted strain); Panel (A), ● YRH1563 (YRH631 + *pho13*Δ), ● YRH2021 (YRH631 + *pbs2*Δ), ● YRH2022 (YRH631 + *pbs2*Δ, *pho13*Δ); Panel (B), ● YRH2056 (CEN.PK2-1C + *pbs2*Δ), ● YRH2057 (CEN.PK2-1C + *pho13*Δ), ● YRH2058 (CEN.PK2-1C + *pbs2*Δ, *pho13*Δ).

3.6. Analysis of *PBS2* and *PHO13* Requirement for Strains Expressing the XR/XDH Pathway

We next investigated whether the causative mutations discovered in the adapted XI-expressing strain were also functional in a strain expressing the XR/XDH pathway. Starting with the CEN.PK2-1C strain, we deleted *PBS2* and *PHO13* in strains engineered to express the *Scheffersomyces stipitis* xylose reductase and xylitol dehydrogenase genes (*XYL1* and *XYL2*), as well as overexpressed *S. cerevisiae* *XKS1*. Contrary to cells expressing the XI pathway, cells expressing the XR/XDH pathway showed a significant improvement in growth from only *PHO13* deletion (YRH2054) (Figure 6). While single deletion of *PBS2* in these cells (YRH2053) did not improve growth on xylose, strain YRH2055 with deletion of both *PBS2* and *PHO13* showed additional improvement in growth compared to the single *PHO13* deletion strain. The implications of this result in comparison to strains expressing the XI/XK pathway are discussed in Section 3.9.

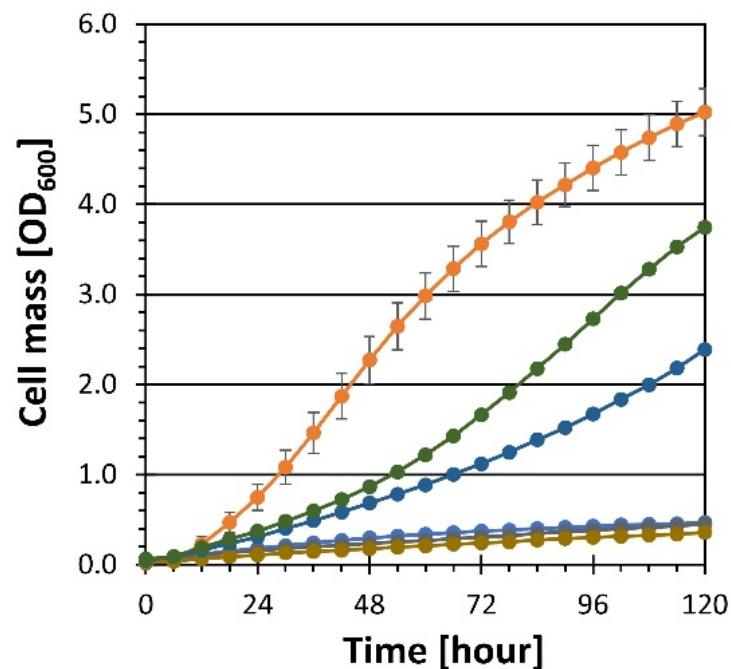


Figure 6. Growth curves for *PBS2* and *PHO13* deletions in strains expressing the XR/XDH pathway. *PBS2* and *PHO13* genes were deleted in strain CEN.PK2-1C expressing the *S. stipitis* *XYL1* and *XYL2*, and *ScXYKS1* genes. YP5X medium was used. Plots are the average values from at least triplicate cultures. Error bars show standard deviations. Scheme 631. (unadapted XI strain), —●— YRH1114 (adapted XI strain), —●— YRH2040 (CEN.PK2-1C with XR/XDH/XK plasmid), —●— YRH2053 (YRH2040 + *pbs2*Δ), —●— YRH2054 (YRH2040 + *pho13*Δ), —●— YRH2055 (YRH2040 + *pbs2*Δ, *pho13*Δ).

3.7. Xylose Fermentation in Strains with Targeted *PBS2* and *PHO13* Deletions

To determine if *PHO13* and *PBS2* mutations were responsible for the increased xylose fermentation observed with the adapted strain YRH1114 in our previous study [16], we determined the effect of both single and double deletion of *PHO13* and *PBS2* in strains expressing either the XI/XK or XR/XDH pathway. Batch fermentations using strains expressing the XI/XK pathway (Figure 7 panels A, C, E, G) were consistent with results from aerobic culture using xylose medium. Single deletion of *PHO13* or *PBS2* did not increase growth or ethanol production when grown under microaerobic conditions.

Deletion of both *PHO13* and *PBS2* resulted in a fermentation profile that was similar to that of the adapted YRH1114 strain (Table 5 and Figure 7). Results from batch fermentations using strains expressing the XR/XDH pathway were also consistent with results from our aerobic growth analyses. As seen under aerobic conditions, single deletion of *PBS2* did not improve fermentation, while single deletion of *PHO13* resulted in a significant increase in xylose consumption and ethanol production (Table 5 and Figure 7 panels B, D, F, H). Strain YRH2055 with deletion of both *PBS2* and *PHO13*, again, showed additional improvement compared to the single *PHO13* deletion strain. As seen previously, using the XR/XDH pathway results in low ethanol yield due to higher levels of xylitol production when compared to strains expressing the XI/XK pathway (Table 5 and [16]). The highest ethanol yields obtained in this study were from the adapted strain (YRH1114) and the strain expressing the XI/XK pathway with targeted deletion of both *PBS2* and *PHO13* (YRH2058). While there was a slight increase in ethanol yield for strain YRH2058 compared to YRH1114, the increase was not statistically significant. Since the fermentation profile of the strain with targeted *PHO13* and *PBS2* deletions was similar to the adapted strain, we believe that mutations to *PHO13* and *PBS2* in YRH1114 are the causative mutations resulting in improved xylose fermentation.

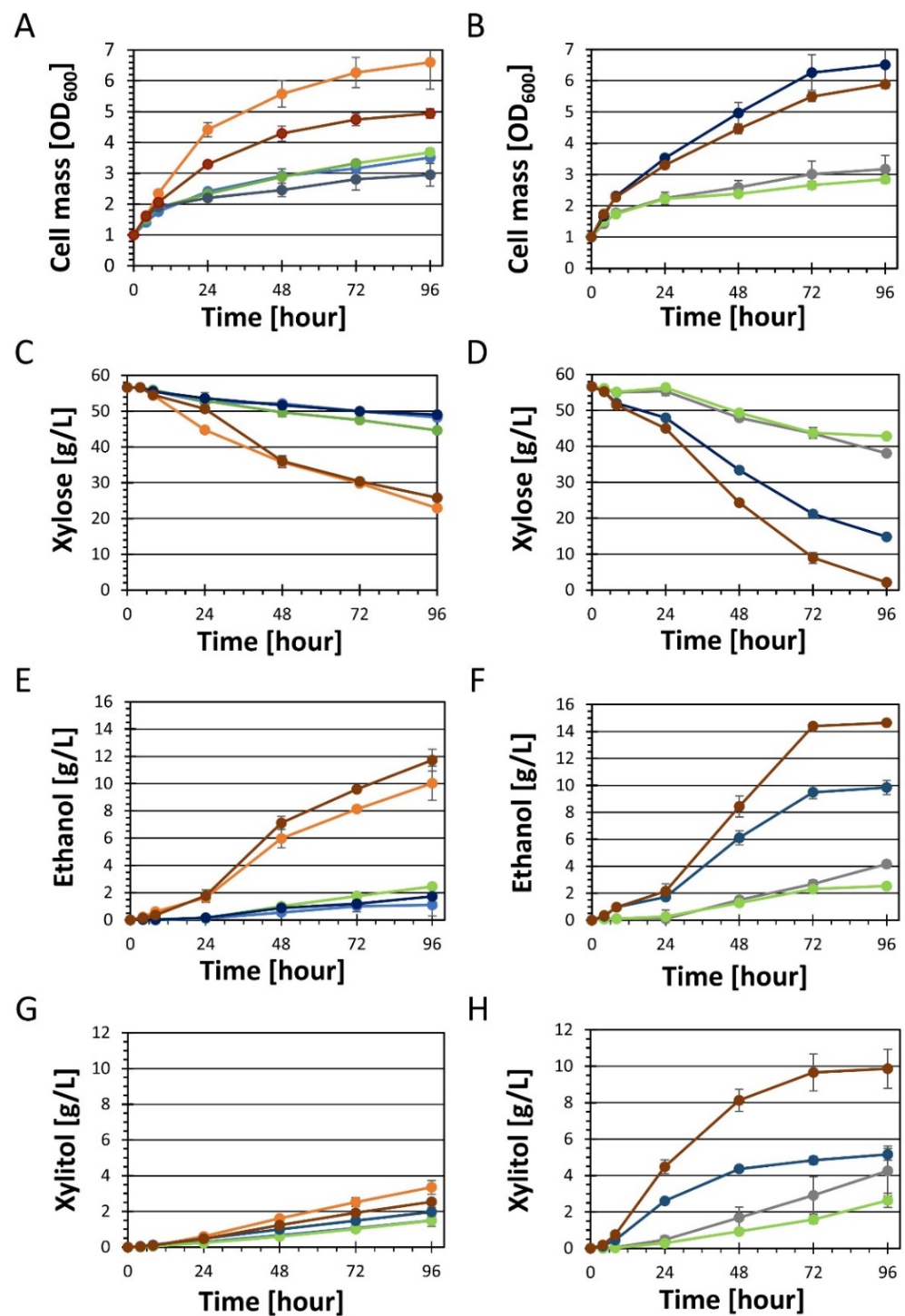


Figure 7. Fermentation analysis for strains with *PBS2* and *PHO13* deletions. (A,C,E,G) CEN.PK2-1C cells expressing *P. ruminicola* XI/XK genes. (B,D,F,H) CEN.PK2-1C expressing the *S. stipitis* *XYL1* and *XYL2*, and *ScXYKS1* genes. YP5X medium was used for all fermentations. Plots are the average values from three biological replicate cultures. Error bars show standard deviations. Strain description: Panels (A,C,E,G) — YRH631 (unadapted XI strain), — YRH1114 (adapted XI strain), — YRH2056 (CEN.PK2-1C + *pbs2*Δ), — YRH2057 (CEN.PK2-1C + *pho13*Δ), — YRH2058 (CEN.PK2-1C + *pbs2*Δ, *pho13*Δ); Panels (B,D,F,H), — YRH2040 (CEN.PK2-1C with XR/XDH/XK plasmid), — YRH2053 (YRH2040 + *pbs2*Δ), — YRH2054 (YRH2040 + *pho13*Δ), — YRH2055 (YRH2040 + *pbs2*Δ, *pho13*Δ).

Table 5. Fermentation of xylose by strains with *PBS2* and *PHO13* deletions.

Strain	Genotype	Xylose Pathway Utilized	Xylose Consumed [g/L]	Final Concentration [g/L]		Specific Consumption or Production Rate [g/g _{CDW} /h]		Ethanol Yield [g _{ethanol} /g _{xylose}]
				Xylitol	Ethanol	Xylose	Ethanol	
YRH631	<i>PHO13</i> , <i>PBS2</i>	XI/XK ^A	8.3 ± 0.81	1.5 ± 0.33	2.3 ± 0.81	0.04 ± 0.003	0.012 ± 0.0066	0.18 ± 0.053
YRH1114	<i>pho13</i> ^{G208C} , <i>pbs2</i> ^{L363X}	XI/XK	33.7 ± 0.60	3.4 ± 0.38	10.0 ± 1.25	0.08 ± 0.011	0.025 ± 0.0064	0.30 ± 0.036
YRH2056	<i>PHO13</i> , <i>pbs2</i> Δ	XI/XK	12.0 ± 0.15	1.5 ± 0.04	2.5 ± 0.07	0.05 ± 0.001	0.011 ± 0.0004	0.20 ± 0.007
YRH2057	<i>pho13</i> Δ, <i>PBS2</i>	XI/XK	7.6 ± 0.18	2.0 ± 0.25	1.7 ± 0.19	0.04 ± 0.005	0.007 ± 0.0051	0.23 ± 0.018
YRH2058	<i>pho13</i> Δ, <i>pbs2</i> Δ	XI/XK	30.8 ± 0.57	2.5 ± 0.01	11.7 ± 0.81	0.10 ± 0.013	0.033 ± 0.0075	0.36 ± 0.036
YRH2040	<i>PHO13</i> , <i>PBS2</i>	XR/XDH/XK _B	18.6 ± 0.30	4.3 ± 1.37	4.2 ± 0.27	0.09 ± 0.012	0.021 ± 0.0030	0.22 ± 0.011
YRH2053	<i>PHO13</i> , <i>pbs2</i> Δ	XR/XDH/XK	13.8 ± 0.54	2.6 ± 0.39	2.5 ± 0.16	0.08 ± 0.004	0.014 ± 0.0010	0.18 ± 0.005
YRH2054	<i>pho13</i> Δ, <i>PBS2</i>	XR/XDH/XK	41.8 ± 0.48	5.2 ± 0.31	9.8 ± 0.52	0.10 ± 0.013	0.025 ± 0.0040	0.24 ± 0.013
YRH2055	<i>pho13</i> Δ, <i>pbs2</i> Δ	XR/XDH/XK	54.5 ± 0.62	9.9 ± 1.06	14.7 ± 0.56	0.15 ± 0.004	0.037 ± 0.0037	0.25 ± 0.027

^A XI/XK genes are from *P. ruminicola*. ^B XR/XDH genes are from *S. stipitis* and the XK gene is from *S. cerevisiae*. Data shown represent the mean values at 96 h from three biological replicates ± standard deviation.

3.8. Mutation to HOG1 Pathway Kinases Improves Xylose Utilization

While this study is the first to show that mutations to *PBS2* can increase xylose utilization, previous studies with strains evolved for improved xylose utilization identified two other members of the mitogen-activated protein (MAP) kinase cascade of which *PBS2* is part. *PBS2* is a MAP kinase kinase (MAPKK) that is part of the high osmolarity glycerol (HOG) pathway (reviewed in [64]). MAP kinase cascades are composed of multiple kinases that transduce environmental signals to the nucleus to regulate gene expression. Depending on the environmental stress, three osmoresponsive MAPKKs (Ste11p, Ssk2p, and Ssk22p) phosphorylate the MAPKK Pbs2p, which in turn, phosphorylates the MAPK Hog1p. Phosphorylated Hog1p translocates to the nucleus and regulates gene expression via its interaction with several transcription factors.

Mutation of the MAPKKK *SSK2* has been found in strains evolved for increased xylose utilization; for example, dos Santos et al. (2016) identified a nonsense mutation in *SSK2* in their evolved strain [35]. The starting parent strain for evolution had multiple copies of the XI gene integrated, as well as multiple genes from the PPP and deletion of *GRE3*. Deletion of *SSK2* in the unevolved parent strain resulted in a significant increase in xylose consumption. Separately, Hou et al., (2016), using a different genetic background and XI gene, also identified a nonsense mutation in the *SSK2* gene of their evolved strain [37]. Again, the unadapted starting parent strain was modified to overexpress XI and PPP genes, as well as deleting *GRE3* and *COX4*. However, validation of the *SSK2* SNP was performed by deletion of *SSK2* in the “clean” parent strain, expressing only the XI gene, not the PPP genes or other deletions. In the clean parent strain, deletion of *SSK2* by itself did not increase xylose utilization. Unfortunately, this study did not delete *SSK2* in the unadapted parent. The differences between these two studies with *SSK2* are consistent with our data for *PBS2* deletion. Deletion of *PBS2*, like deletion of *SSK2*, is only beneficial when PPP activity is increased. In our strain, this was implemented by deleting *PHO13*.

Mutations in the MAPK *HOG1* were also previously identified in screens for enhanced xylose utilization [17]. We believe that *PBS2* deletion (and possibly *SSK2* deletion) likely mimics a *HOG1* deletion. Phenotypes of mutant *PBS2* and *HOG1* strains are identical, and gene expression patterns from strains with either *PBS2* or *HOG1* deletion are almost identical [65]. *HOG1* is required for *GRE3* expression [66,67] and part of the increase in xylose utilization due to *HOG1* mutation has been attributed to a reduction in *GRE3*

expression [17,34]. Gre3p is an endogenous xylose reductase, and deletion of *GRE3* has been shown to decrease production of xylitol 2- to 3-fold in XI expressing strains [68]. Xylitol is also a competitive inhibitor of xylose isomerase, so decreased xylitol concentration leads to increased XI activity [12,69]. Consistent with decreased Gre3p and decreased xylose reductase activity, we previously showed that our adapted strain has 2.9-fold increased XI activity and a 1.7-fold decrease in xylitol yield compared to the unadapted strain [16]. Batch fermentations performed in this study also showed a 1.8-fold and 2.2-fold decrease in xylitol yield for the adapted YRH1114 strain and YRH2058 (CEN.PK2-1C with XI/XK pathway + *pbs2*Δ, *pho13*Δ) when compared to the unadapted strain, respectively.

3.9. Model Showing Involvement of *PBS2* and *PHO13* in Separate Steps of Xylose Utilization

We propose the following model to explain the requirement of both *pbs2* and *pho13* mutation to improve xylose growth for the engineered strains used in this study (Figure 8). Loss of *PHO13* function has been shown to increase expression of PPP enzymes [31], which is required for general xylose metabolism. For strains expressing the XI pathway, cells with just *pho13*Δ are still limited in xylose conversion to X5P (Figure 8A). Cells with *pbs2*Δ, which likely acts like a *hog1*Δ strain because *PBS2* is required for *HOG1* function [65], have increased xylose conversion to X5P, but are then limited by poor flux through the PPP due to the presence of *PHO13*. When utilizing the XI pathway, both gene deletions are required to get xylose into central metabolism and allow cell growth. Conversely, for cells expressing the XR/XDH pathway for xylose metabolism, X5P production is not as limiting a factor. Thus, increased flux through the PPP from deletion of only *PHO13* would be expected to increase growth on xylose (Figure 8B). Previous studies using multiple different genetic backgrounds are consistent with this model. These studies show that deleting only *PHO13* in strains using the XR/XDH pathway increases xylose utilization [31–33,40,70]. Several of these studies utilized different genetic backgrounds. Different XI and XK genes were also used compared to ours, suggesting that the results with respect to *PHO13* deletion are not unique to specific strain backgrounds or xylose isomerases.

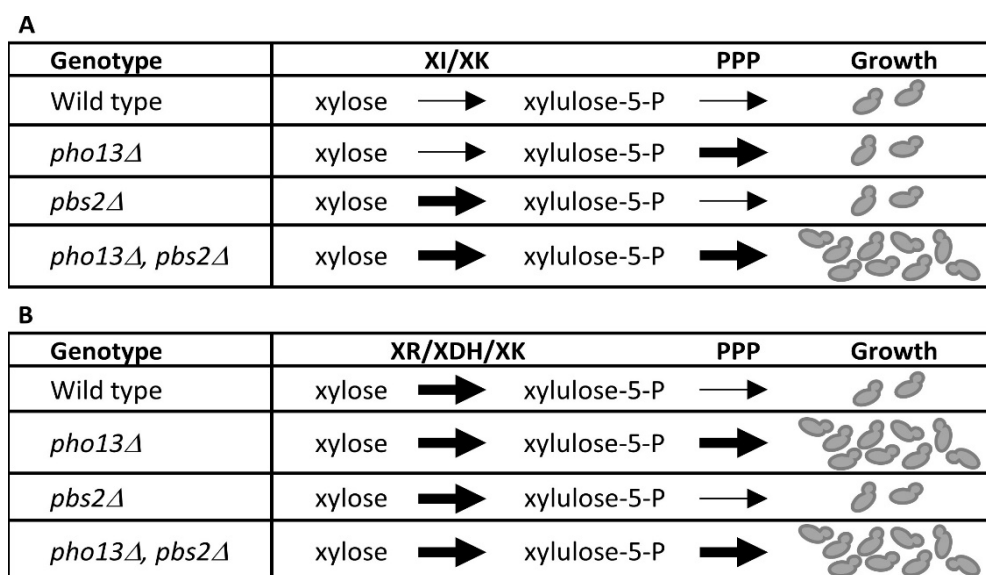


Figure 8. Proposed model showing involvement of *PBS2* and *PHO13* in xylose metabolism. (A) Cells expressing the XI/XK pathway (CEN.PK2-1C cells overexpressing *P. ruminicola* XI and XK) are limited in conversion of xylose to xylulose-5-P and require deletion of both *PBS2* and *PHO13* for improved xylose utilization. (B) Cells expressing the XR/XDH pathway (CEN.PK2-1C cells overexpressing *S. stipitis* XR and XDH with *S. cerevisiae* XK) are not as limited in xylulose-5-P production and show improved xylose utilization in strains with only the *PHO13* deletion.

Strains lacking *PBS2* or *HOG1*, although beneficial for xylose utilization, may not be ideal for growth in lignocellulosic hydrolysates. For example, CRISPRi-identified downregulation of both *HOG1* and *PBS2* was linked to poor growth in spruce hydrolysate [71]. *HOG1* deletion was also shown to affect glucose utilization in corn stover hydrolysate [72]. The adapted YRH1114 strain was previously tested on a glucose and xylose mixture, and glucose utilization was not decreased [16]. However, hydrolysate was not used in the previous study. There is some evidence that *PBS2* and *HOG1* deletions may not be completely identical. Autophosphorylation of Hog1p has been shown to occur in a *pbs2* Δ strain [73]. In this regard, deletion of *PBS2*, or co-expression of the *pbs2*^{L363X} allele with *PBS2*, may yield better results than *HOG1* deletion, since some level of Hog1p phosphorylation would still be present in these strains. Additional work is needed to determine if there are differences between *HOG1* and *PBS2* deletions, as well as comparison of *PBS2* deletion and the semi-dominant *pbs2*^{L363X} allele for negative effects when grown on lignocellulosic hydrolysates.

4. Conclusions

In the present work, we analyzed the genome sequence of an engineered *S. cerevisiae* strain expressing codon-optimized *Prevotella ruminicola* XI and XK genes that was previously adapted for increased xylose fermentation [16]. Tetrad analysis of haploid spores from the heterozygous diploid showed that of the seven ORF mutations present in the adapted strain, only *pbs2*^{L363X} and *pho13*^{G208C} mutations improved xylose utilization. Strains carrying a single mutated or deleted *PBS2* or *PHO13* did not show improved growth on xylose, indicating that both mutations were necessary. Double deletion of *PBS2* and *PHO13* also improved xylose utilization for strains expressing the XR/XDH pathway. However, unlike strains expressing the XI pathway, these strains also showed a significant improvement from deletion of the *PHO13* gene alone.

Supplementary Materials: The following supporting information can be downloaded at <https://www.mdpi.com/article/10.3390/fermentation8120669/s1>: Table S1: DNA oligonucleotides used in this study; Construction of plasmids for expressing *PBS2* and *PHO13*; Construction of *PBS2* and *PHO13* deletion strains.

Author Contributions: Conceptualization, R.E.H. and J.A.M.; investigation, methodology, and formal analysis, R.E.H., J.A.M. and N.N.N.; writing—original draft preparation, R.E.H.; writing—reviewing, and editing, R.E.H., J.A.M. and N.N.N. All authors have read and agreed to the published version of the manuscript.

Funding: This research was supported by the US Department of Agriculture, Agricultural Research Service. Mention of trade names or commercial products in this article is solely for the purpose of providing scientific information and does not imply recommendation or endorsement by the US Department of Agriculture. USDA is an equal opportunity provider and employer. This article is a US Government work and is in the public domain in the USA.

Informed Consent Statement: Not applicable.

Data Availability Statement: All DNA sequence reads have been deposited in the NCBI Sequence Read Archive (SRA) under BioProject PRJNA877627.

Acknowledgments: We thank Katherine Card and Sarah Frazer for technical assistance throughout this study.

Conflicts of Interest: The authors declare no conflict of interest.

References

1. Nevoigt, E. Progress in metabolic engineering of *Saccharomyces cerevisiae*. *Microbiol. Mol. Biol. Rev.* **2008**, *72*, 379–412. [[CrossRef](#)] [[PubMed](#)]
2. Jansen, M.L.A.; Bracher, J.M.; Papapetridis, I.; Verhoeven, M.D.; de Bruijn, H.; de Waal, P.P.; van Maris, A.J.A.; Klaassen, P.; Pronk, J.T. *Saccharomyces cerevisiae* strains for second-generation ethanol production: From academic exploration to industrial implementation. *FEMS Yeast Res.* **2017**, *17*, fox044. [[CrossRef](#)] [[PubMed](#)]

3. Lee, J.W.; Yook, S.; Koh, H.; Rao, C.V.; Jin, Y.S. Engineering xylose metabolism in yeasts to produce biofuels and chemicals. *Curr. Opin. Biotechnol.* **2021**, *67*, 15–25. [[CrossRef](#)] [[PubMed](#)]
4. Jordan, D.B.; Bowman, M.J.; Braker, J.D.; Dien, B.S.; Hector, R.E.; Lee, C.C.; Mertens, J.A.; Wagschal, K. Plant cell walls to ethanol. *Biochem. J.* **2012**, *442*, 241–252. [[CrossRef](#)]
5. Borgstrom, C.; Wasserstrom, L.; Almqvist, H.; Broberg, K.; Klein, B.; Noack, S.; Liden, G.; Gorwa-Grauslund, M.F. Identification of modifications procuring growth on xylose in recombinant *Saccharomyces cerevisiae* strains carrying the Weimberg pathway. *Metab. Eng.* **2019**, *55*, 1–11. [[CrossRef](#)]
6. Kotter, P.; Ciriacy, M. Xylose Fermentation by *Saccharomyces cerevisiae*. *Appl. Microbiol. Biotechnol.* **1993**, *38*, 776–783. [[CrossRef](#)]
7. Bruinenberg, P.M.; de Bot, P.H.M.; van Dijken, J.P.; Scheffers, W.A. The role of redox balances in the anaerobic fermentation of xylose by yeasts. *Eur. J. Appl. Microbiol. Biotechnol.* **1983**, *18*, 287–292. [[CrossRef](#)]
8. van Maris, A.J.; Winkler, A.A.; Kuyper, M.; de Laat, W.T.; van Dijken, J.P.; Pronk, J.T. Development of efficient xylose fermentation in *Saccharomyces cerevisiae*: Xylose isomerase as a key component. *Adv. Biochem. Eng. Biotechnol.* **2007**, *108*, 179–204. [[CrossRef](#)]
9. Harhangi, H.R.; Akhmanova, A.S.; Emmens, R.; van der Drift, C.; de Laat, W.T.; van Dijken, J.P.; Jetten, M.S.; Pronk, J.T.; Op den Camp, H.J. Xylose metabolism in the anaerobic fungus *Piromyces* sp. strain E2 follows the bacterial pathway. *Arch. Microbiol.* **2003**, *180*, 134–141. [[CrossRef](#)]
10. Gardonyi, M.; Hahn-Hagerdal, B. The *Streptomyces rubiginosus* xylose isomerase is misfolded when expressed in *Saccharomyces cerevisiae*. *Enzym. Microb. Technol.* **2003**, *32*, 252–259. [[CrossRef](#)]
11. Kuyper, M.; Hartog, M.M.; Toirkens, M.J.; Almering, M.J.; Winkler, A.A.; van Dijken, J.P.; Pronk, J.T. Metabolic engineering of a xylose-isomerase-expressing *Saccharomyces cerevisiae* strain for rapid anaerobic xylose fermentation. *FEMS Yeast Res.* **2005**, *5*, 399–409. [[CrossRef](#)] [[PubMed](#)]
12. Brat, D.; Boles, E.; Wiedemann, B. Functional expression of a bacterial xylose isomerase in *Saccharomyces cerevisiae*. *Appl. Environ. Microbiol.* **2009**, *75*, 2304–2311. [[CrossRef](#)] [[PubMed](#)]
13. Madhavan, A.; Tamalampudi, S.; Ushida, K.; Kanai, D.; Katahira, S.; Srivastava, A.; Fukuda, H.; Bisaria, V.S.; Kondo, A. Xylose isomerase from polycentric fungus *Orpinomyces*: Gene sequencing, cloning, and expression in *Saccharomyces cerevisiae* for bioconversion of xylose to ethanol. *Appl. Microbiol. Biotechnol.* **2009**, *82*, 1067–1078. [[CrossRef](#)] [[PubMed](#)]
14. Zhou, H.; Cheng, J.S.; Wang, B.L.; Fink, G.R.; Stephanopoulos, G. Xylose isomerase overexpression along with engineering of the pentose phosphate pathway and evolutionary engineering enable rapid xylose utilization and ethanol production by *Saccharomyces cerevisiae*. *Metab. Eng.* **2012**, *14*, 611–622. [[CrossRef](#)]
15. Bamba, T.; Hasunuma, T.; Kondo, A. Disruption of *PHO13* improves ethanol production via the xylose isomerase pathway. *AMB Express* **2016**, *6*, 4. [[CrossRef](#)]
16. Hector, R.E.; Dien, B.S.; Cotta, M.A.; Mertens, J.A. Growth and fermentation of D-xylose by *Saccharomyces cerevisiae* expressing a novel D-xylose isomerase originating from the bacterium *Prevotella ruminicola* TC2-24. *Biotechnol. Biofuels* **2013**, *6*, 84. [[CrossRef](#)] [[PubMed](#)]
17. Sato, T.K.; Tremaine, M.; Parreiras, L.S.; Hebert, A.S.; Myers, K.S.; Higbee, A.J.; Sardi, M.; McIlwain, S.J.; Ong, I.M.; Breuer, R.J.; et al. Directed evolution reveals unexpected epistatic interactions that alter metabolic regulation and enable anaerobic xylose use by *Saccharomyces cerevisiae*. *PLoS Genet.* **2016**, *12*, e1006372. [[CrossRef](#)]
18. Kuyper, M.; Toirkens, M.J.; Diderich, J.A.; Winkler, A.A.; van Dijken, J.P.; Pronk, J.T. Evolutionary engineering of mixed-sugar utilization by a xylose-fermenting *Saccharomyces cerevisiae* strain. *FEMS Yeast Res.* **2005**, *5*, 925–934. [[CrossRef](#)] [[PubMed](#)]
19. Garcia Sanchez, R.; Karhumaa, K.; Fonseca, C.; Sanchez Nogue, V.; Almeida, J.R.; Larsson, C.U.; Bengtsson, O.; Bettiga, M.; Hahn-Hägerdal, B.; Gorwa-Grauslund, M.F. Improved xylose and arabinose utilization by an industrial recombinant *Saccharomyces cerevisiae* strain using evolutionary engineering. *Biotechnol. Biofuels* **2010**, *3*, 13. [[CrossRef](#)]
20. Lee, S.-M.; Jellison, T.; Alper, H.S. Systematic and evolutionary engineering of a xylose isomerase-based pathway in *Saccharomyces cerevisiae* for efficient conversion yields. *Biotechnol. Biofuels* **2014**, *7*, 122. [[CrossRef](#)]
21. Tomas-Pejo, E.; Ballesteros, M.; Oliva, J.M.; Olsson, L. Adaptation of the xylose fermenting yeast *Saccharomyces cerevisiae* F12 for improving ethanol production in different fed-batch SSF processes. *J. Ind. Microbiol. Biotechnol.* **2010**, *37*, 1211–1220. [[CrossRef](#)] [[PubMed](#)]
22. Shen, Y.; Chen, X.; Peng, B.; Chen, L.; Hou, J.; Bao, X. An efficient xylose-fermenting recombinant *Saccharomyces cerevisiae* strain obtained through adaptive evolution and its global transcription profile. *Appl. Microbiol. Biotechnol.* **2012**, *96*, 1079–1091. [[CrossRef](#)]
23. Kuyper, M.; Winkler, A.A.; van Dijken, J.P.; Pronk, J.T. Minimal metabolic engineering of *Saccharomyces cerevisiae* for efficient anaerobic xylose fermentation: A proof of principle. *FEMS Yeast Res.* **2004**, *4*, 655–664. [[CrossRef](#)] [[PubMed](#)]
24. Peng, B.; Shen, Y.; Li, X.; Chen, X.; Hou, J.; Bao, X. Improvement of xylose fermentation in respiratory-deficient xylose-fermenting *Saccharomyces cerevisiae*. *Metab. Eng.* **2012**, *14*, 9–18. [[CrossRef](#)] [[PubMed](#)]
25. Sonderegger, M.; Sauer, U. Evolutionary engineering of *Saccharomyces cerevisiae* for anaerobic growth on xylose. *Appl. Environ. Microbiol.* **2003**, *69*, 1990–1998. [[CrossRef](#)] [[PubMed](#)]
26. Wisselink, H.W.; Toirkens, M.J.; Wu, Q.; Pronk, J.T.; van Maris, A.J. Novel evolutionary engineering approach for accelerated utilization of glucose, xylose, and arabinose mixtures by engineered *Saccharomyces cerevisiae* strains. *Appl. Environ. Microbiol.* **2009**, *75*, 907–914. [[CrossRef](#)] [[PubMed](#)]

27. Smith, J.; van Rensburg, E.; Gorgens, J.F. Simultaneously improving xylose fermentation and tolerance to lignocellulosic inhibitors through evolutionary engineering of recombinant *Saccharomyces cerevisiae* harbouring xylose isomerase. *BMC Biotechnol.* **2014**, *14*, 41. [[CrossRef](#)]
28. Scalcinati, G.; Otero, J.M.; Van Vleet, J.R.; Jeffries, T.W.; Olsson, L.; Nielsen, J. Evolutionary engineering of *Saccharomyces cerevisiae* for efficient aerobic xylose consumption. *FEMS Yeast Res.* **2012**, *12*, 582–597. [[CrossRef](#)]
29. Demeke, M.M.; Dietz, H.; Li, Y.; Foulquie-Moreno, M.R.; Mutturi, S.; Deprez, S.; Den Abt, T.; Bonini, B.M.; Liden, G.; Dumortier, F.; et al. Development of a D-xylose fermenting and inhibitor tolerant industrial *Saccharomyces cerevisiae* strain with high performance in lignocellulose hydrolysates using metabolic and evolutionary engineering. *Biotechnol. Biofuels* **2013**, *6*, 89. [[CrossRef](#)]
30. Matsushika, A.; Oguri, E.; Sawayama, S. Evolutionary adaptation of recombinant shochu yeast for improved xylose utilization. *J. Biosci. Bioeng.* **2010**, *110*, 102–105. [[CrossRef](#)]
31. Kim, S.R.; Xu, H.; Lesmana, A.; Kuzmanovic, U.; Au, M.; Florencia, C.; Oh, E.J.; Zhang, G.; Kim, K.H.; Jin, Y.S. Deletion of *PHO13*, encoding haloacid dehalogenase type IIA phosphatase, results in upregulation of the pentose phosphate pathway in *Saccharomyces cerevisiae*. *Appl. Environ. Microbiol.* **2015**, *81*, 1601–1609. [[CrossRef](#)]
32. Ni, H.; Laplaza, J.M.; Jeffries, T.W. Transposon mutagenesis to improve the growth of recombinant *Saccharomyces cerevisiae* on D-xylose. *Appl. Environ. Microbiol.* **2007**, *73*, 2061–2066. [[CrossRef](#)] [[PubMed](#)]
33. Kim, S.R.; Skerker, J.M.; Kang, W.; Lesmana, A.; Wei, N.; Arkin, A.P.; Jin, Y.S. Rational and Evolutionary Engineering Approaches Uncover a Small Set of Genetic Changes Efficient for Rapid Xylose Fermentation in *Saccharomyces cerevisiae*. *PLoS ONE* **2013**, *8*, e57048. [[CrossRef](#)]
34. Parreiras, L.S.; Breuer, R.J.; Avanasani Narasimhan, R.; Higbee, A.J.; La Reau, A.; Tremaine, M.; Qin, L.; Willis, L.B.; Bice, B.D.; Bonfert, B.L.; et al. Engineering and two-stage evolution of a lignocellulosic hydrolysate-tolerant *Saccharomyces cerevisiae* strain for anaerobic fermentation of xylose from AFEX pretreated corn stover. *PLoS ONE* **2014**, *9*, e107499. [[CrossRef](#)] [[PubMed](#)]
35. Dos Santos, L.V.; Carazzolle, M.F.; Nagamatsu, S.T.; Sampaio, N.M.V.; Almeida, L.D.; Pirolla, R.A.S.; Borelli, G.; Corrêa, T.L.R.; Argueso, J.L.; Pereira, G.A.G. Unraveling the genetic basis of xylose consumption in engineered *Saccharomyces cerevisiae* strains. *Sci. Rep.* **2016**, *6*, 38676. [[CrossRef](#)] [[PubMed](#)]
36. Lee, S.B.; Tremaine, M.; Place, M.; Liu, L.; Pier, A.; Krause, D.J.; Xie, D.; Zhang, Y.; Landick, R.; Gasch, A.P.; et al. Crabtree/Warburg-like aerobic xylose fermentation by engineered *Saccharomyces cerevisiae*. *Metab. Eng.* **2021**, *68*, 119–130. [[CrossRef](#)]
37. Hou, J.; Jiao, C.; Peng, B.; Shen, Y.; Bao, X. Mutation of a regulator Ask10p improves xylose isomerase activity through up-regulation of molecular chaperones in *Saccharomyces cerevisiae*. *Metab. Eng.* **2016**, *38*, 241–250. [[CrossRef](#)]
38. Papapetridis, I.; Verhoeven, M.D.; Wiersma, S.J.; Goudriaan, M.; van Maris, A.J.A.; Pronk, J.T. Laboratory evolution for forced glucose-xylose co-consumption enables identification of mutations that improve mixed-sugar fermentation by xylose-fermenting *Saccharomyces cerevisiae*. *FEMS Yeast Res.* **2018**, *18*, foy056. [[CrossRef](#)]
39. Verhoeven, M.D.; Lee, M.; Kamoen, L.; van den Broek, M.; Janssen, D.B.; Daran, J.-M.G.; van Maris, A.J.A.; Pronk, J.T. Mutations in *PMR1* stimulate xylose isomerase activity and anaerobic growth on xylose of engineered *Saccharomyces cerevisiae* by influencing manganese homeostasis. *Sci. Rep.* **2017**, *7*, 46155. [[CrossRef](#)]
40. Jeong, D.; Oh, E.J.; Ko, J.K.; Nam, J.O.; Park, H.S.; Jin, Y.S.; Lee, E.J.; Kim, S.R. Metabolic engineering considerations for the heterologous expression of xylose-catabolic pathways in *Saccharomyces cerevisiae*. *PLoS ONE* **2020**, *15*, e0236294. [[CrossRef](#)]
41. Demeke, M.M.; Foulquie-Moreno, M.R.; Dumortier, F.; Thevelein, J.M. Rapid evolution of recombinant *Saccharomyces cerevisiae* for Xylose fermentation through formation of extra-chromosomal circular DNA. *PLoS Genet.* **2015**, *11*, e1005010. [[CrossRef](#)]
42. Hector, R.E.; Mertens, J.A.; Nichols, N.N. Development and characterization of vectors for tunable expression of both xylose-regulated and constitutive gene expression in *Saccharomyces* yeasts. *New Biotechnol.* **2019**, *53*, 16–23. [[CrossRef](#)]
43. Christianson, T.W.; Sikorski, R.S.; Dante, M.; Shero, J.H.; Hieter, P. Multifunctional yeast high-copy-number shuttle vectors. *Gene* **1992**, *110*, 119–122. [[CrossRef](#)] [[PubMed](#)]
44. Bennett, C.B.; Lewis, A.L.; Baldwin, K.K.; Resnick, M.A. Lethality induced by a single site-specific double-strand break in a dispensable yeast plasmid. *Proc. Natl. Acad. Sci. USA* **1993**, *90*, 5613–5617. [[CrossRef](#)] [[PubMed](#)]
45. Hector, R.E.; Dien, B.S.; Cotta, M.A.; Qureshi, N. Engineering industrial *Saccharomyces cerevisiae* strains for xylose fermentation and comparison for switchgrass conversion. *J. Ind. Microbiol. Biotechnol.* **2011**, *38*, 1193–1202. [[CrossRef](#)]
46. Hector, R.E.; Mertens, J.A.; Bowman, M.J.; Nichols, N.N.; Cotta, M.A.; Hughes, S.R. *Saccharomyces cerevisiae* engineered for xylose metabolism requires gluconeogenesis and the oxidative branch of the pentose phosphate pathway for aerobic xylose assimilation. *Yeast* **2011**, *28*, 645–660. [[CrossRef](#)]
47. Hauf, J.; Zimmermann, F.K.; Muller, S. Simultaneous genomic overexpression of seven glycolytic enzymes in the yeast *Saccharomyces cerevisiae*. *Enzym. Microb. Technol.* **2000**, *26*, 688–698. [[CrossRef](#)] [[PubMed](#)]
48. Mertens, J.A.; Kelly, A.; Hector, R.E. Screening for inhibitor tolerant *Saccharomyces cerevisiae* strains from diverse environments for use as platform strains for production of fuels and chemicals from biomass. *Bioresour. Technol. Rep.* **2018**, *3*, 154–161. [[CrossRef](#)]
49. Huxley, C.; Green, E.D.; Dunham, I. Rapid assessment of *S. cerevisiae* mating type by PCR. *Trends Genet.* **1990**, *6*, 236. [[CrossRef](#)]
50. Chen, J.; Schedl, T. A simple one-step PCR assay for SNP detection. *MicroPubl. Biol.* **2021**, 1–4. [[CrossRef](#)]
51. Nichols, N.N.; Hector, R.E.; Saha, B.C.; Frazer, S.E.; Kennedy, G.J. Biological abatement of inhibitors in rice hull hydrolyzate and fermentation to ethanol using conventional and engineered microbes. *Biomass Bioenergy* **2014**, *67*, 79–88. [[CrossRef](#)]
52. Araya, C.L.; Payen, C.; Dunham, M.J.; Fields, S. Whole-genome sequencing of a laboratory-evolved yeast strain. *BMC Genom.* **2010**, *11*, 88. [[CrossRef](#)] [[PubMed](#)]

53. Kondrashov, F.A. Gene duplication as a mechanism of genomic adaptation to a changing environment. *Proc. R. Soc. Lond. Ser. B Biol. Sci.* **2012**, *279*, 5048–5057. [[CrossRef](#)] [[PubMed](#)]
54. Ames, R.M.; Rash, B.M.; Hentges, K.E.; Robertson, D.L.; Delneri, D.; Lovell, S.C. Gene duplication and environmental adaptation within yeast populations. *Genome Biol. Evol.* **2010**, *2*, 591–601. [[CrossRef](#)]
55. Jin, Y.S.; Ni, H.; Laplaza, J.M.; Jeffries, T.W. Optimal growth and ethanol production from xylose by recombinant *Saccharomyces cerevisiae* require moderate D-xylulokinase activity. *Appl. Environ. Microbiol.* **2003**, *69*, 495–503. [[CrossRef](#)]
56. Johansson, B.; Christensson, C.; Hobbey, T.; Hahn-Hagerdal, B. Xylulokinase overexpression in two strains of *Saccharomyces cerevisiae* also expressing xylose reductase and xylitol dehydrogenase and its effect on fermentation of xylose and lignocellulosic hydrolysate. *Appl. Environ. Microbiol.* **2001**, *67*, 4249–4255. [[CrossRef](#)]
57. Rodriguez-Peña, J.M.; Cid, V.J.; Arroyo, J.; Nombela, C. The YGR194c (XKS1) gene encodes the xylulokinase from the budding yeast *Saccharomyces cerevisiae*. *FEMS Microbiol. Lett.* **1998**, *162*, 155–160. [[CrossRef](#)]
58. Deng, X.X.; Ho, N.W. Xylulokinase activity in various yeasts including *Saccharomyces cerevisiae* containing the cloned xylulokinase gene. Scientific note. *Appl. Biochem. Biotechnol.* **1990**, *24*, 193–199. [[CrossRef](#)]
59. Matsushika, A.; Sawayama, S. Comparative study on a series of recombinant flocculent *Saccharomyces cerevisiae* strains with different expression levels of xylose reductase and xylulokinase. *Enzym. Microb. Technol.* **2011**, *48*, 466–471. [[CrossRef](#)]
60. Krieger, F.; Moglich, A.; Kiefhaber, T. Effect of proline and glycine residues on dynamics and barriers of loop formation in polypeptide chains. *J. Am. Chem. Soc.* **2005**, *127*, 3346–3352. [[CrossRef](#)]
61. Jumper, J.; Evans, R.; Pritzel, A.; Green, T.; Figurnov, M.; Ronneberger, O.; Tunyasuvunakool, K.; Bates, R.; Zidek, A.; Potapenko, A.; et al. Highly accurate protein structure prediction with AlphaFold. *Nature* **2021**, *596*, 583–589. [[CrossRef](#)] [[PubMed](#)]
62. Varadi, M.; Anyango, S.; Deshpande, M.; Nair, S.; Natassia, C.; Yordanova, G.; Yuan, D.; Stroe, O.; Wood, G.; Laydon, A.; et al. AlphaFold Protein Structure Database: Massively expanding the structural coverage of protein-sequence space with high-accuracy models. *Nucleic Acids Res.* **2022**, *50*, D439–D444. [[CrossRef](#)] [[PubMed](#)]
63. Murakami, Y.; Tatebayashi, K.; Saito, H. Two adjacent docking sites in the yeast Hog1 mitogen-activated protein (MAP) kinase differentially interact with the Pbs2 MAP kinase kinase and the Ptp2 protein tyrosine phosphatase. *Mol. Cell. Biol.* **2008**, *28*, 2481–2494. [[CrossRef](#)] [[PubMed](#)]
64. Saito, H.; Posas, F. Response to hyperosmotic stress. *Genetics* **2012**, *192*, 289–318. [[CrossRef](#)] [[PubMed](#)]
65. O'Rourke, S.M.; Herskowitz, I. Unique and redundant roles for HOG MAPK pathway components as revealed by whole-genome expression analysis. *Mol. Biol. Cell* **2004**, *15*, 532–542. [[CrossRef](#)]
66. Aguilera, J.; Rodriguez-Vargas, S.; Prieto, J.A. The HOG MAP kinase pathway is required for the induction of methylglyoxal-responsive genes and determines methylglyoxal resistance in *Saccharomyces cerevisiae*. *Mol. Microbiol.* **2005**, *56*, 228–239. [[CrossRef](#)] [[PubMed](#)]
67. Garay-Arroyo, A.; Covarrubias, A.A. Three genes whose expression is induced by stress in *Saccharomyces cerevisiae*. *Yeast* **1999**, *15*, 879–892. [[CrossRef](#)]
68. Träff, K.L.; Otero Cordero, R.R.; van Zyl, W.H.; Hahn-Hägerdal, B. Deletion of the GRE3 aldose reductase gene and its influence on xylose metabolism in recombinant strains of *Saccharomyces cerevisiae* expressing the *xylA* and *XKS1* genes. *Appl. Environ. Microbiol.* **2001**, *67*, 5668–5674. [[CrossRef](#)] [[PubMed](#)]
69. Kovalevsky, A.; Hanson, B.L.; Mason, S.A.; Forsyth, V.T.; Fisher, Z.; Mustyakimov, M.; Blakeley, M.P.; Keen, D.A.; Langan, P. Inhibition of D-xylose isomerase by polyols: Atomic details by joint X-ray/neutron crystallography. *Acta Crystallogr. D* **2012**, *68*, 1201–1206. [[CrossRef](#)]
70. Van Vleet, J.H.; Jeffries, T.W.; Olsson, L. Deleting the para-nitrophenyl phosphatase (pNPPase), *PHO13*, in recombinant *Saccharomyces cerevisiae* improves growth and ethanol production on D-xylose. *Metab. Eng.* **2008**, *10*, 360–369. [[CrossRef](#)]
71. Gutmann, F.; Jann, C.; Pereira, F.; Johansson, A.; Steinmetz, L.M.; Patil, K.R. CRISPRi screens reveal genes modulating yeast growth in lignocellulose hydrolysate. *Biotechnol. Biofuels* **2021**, *14*, 41. [[CrossRef](#)] [[PubMed](#)]
72. Wagner, E.R.; Myers, K.S.; Riley, N.M.; Coon, J.J.; Gasch, A.P. PKA and HOG signaling contribute separable roles to anaerobic xylose fermentation in yeast engineered for biofuel production. *PLoS ONE* **2019**, *14*, e0212389. [[CrossRef](#)] [[PubMed](#)]
73. Maayan, I.; Beenstock, J.; Marbach, I.; Tabachnick, S.; Livnah, O.; Engelberg, D. Osmostress induces autophosphorylation of Hog1 via a C-terminal regulatory region that is conserved in p38alpha. *PLoS ONE* **2012**, *7*, e44749. [[CrossRef](#)] [[PubMed](#)]